Enhancement in Rejected Heat from Heat Sinks Using High Flexible Winglets with Large Deformation and Low Blockage Effect

S. A. Gandjalikhan Nassab*

Department of Mechanical Engineering, Shahid Bahonar University of Kerman, Kerman, Iran

PAPER INFO

A B S T R A C T

This paper presents an original concept of using high flexible flapping vortex generator in a heat sink for airside heat transfer augmentation. The proposed thin winglet, made with an elastic sheet, is responsible for increasing the cooling rate and mixing quality performance in laminar convection airflow. This study focuses on the excessive bending of the flapping winglet and reducing its blockage effect and pressure drop. This novel concept is demonstrated using a numerical simulation of the flow field with a coupled Fluid-Solid-Interaction technique in transient conditions. The continuity, momentum, and energy equations for forced convection airflow are solved by the finite element method using the COMSOL Multi-physics. Numerical results reveal high amplitude for the flapping vortex generator while under a large deformation and bending. This behavior leads to flow mixing with a small blockage effect due to the deformed aerodynamic shape of the winglet. The present findings show that the high flexible winglet enhances the rejected heat by 100%, with a 33% decrease in pressure drop compared to the rigid vortex generator at the same air velocity.

doi: 10.5829/ijee.2022.13.01.02

NOMENCLATURE

c_p	Specific heat (kj/kg K)		**Greek symbols**
E	Module of elasticity (Pa)	α	Thermal diffusivity (m^2/s)
H	Thickness of the air layer (m)	β	Attacked angle (degree)
h	Convection coefficient (W/m^2 K)	λ	Lame's first parameter (Pa)
k	Thermal conductivity (W/m K)	τ	Time period (s)
L	Length of heat sink (m)	μ_s	Lame's second parameter (Pa)
Nu	Nusselt number	μ	Viscosity (kg/m s)
Pr	Prandtl number	ρ	Density (kg/m^3)
Re	Reynolds number		**Subscript**
t	Time (s)	amb	Ambient
T	Temperature (K)	conv	Convection
(u, v)	x- and y- velocity components (m/s)	in	Inlet
U	Time average flow velocity (m/s)	i, j	Indices in tensor notation
U_s	Displacement vector of VG (mm)	m	Mean bulk
(x, y)	Vertical and horizontal coordinates (m)	s	Solid
x_0	Axial location of VG (m)	w	Wall

*Corresponding Author Email: ganj110@uk.ac.ir (S. A. Gandjalikhan Nassab)

INTRODUCTION

In recent years, several countries have experienced limited freshwater due to the fast-growing population. Increasing the dry cooling ratio in many thermal systems such as thermoelectric power generators could save a considerable amount of freshwater. On the other hand, the airside convective heat transfer coefficient is about two orders of magnitude lower than water. Also, dry cooling requires higher pumping power and surface heat transfer to have the same cooling rate as wet cooling. So, enhancement in convection coefficient is very important to make dry cooling more widespread. Much attention has been paid on this subject by many researchers up to now [1].

Through experimental and numerical work, the enhancement of thermo-hydraulic performance of solar air heaters (SAHs) was investigated by employing convex and concave channels for different curvature angles from 25 to 50° [2]. Numerical findings for convex and concave designs displayed 43% and 31% thermally more effective compared to conventional SAHs. The same authors also numerically investigated curved and flat SAHs under different environmental circumstances while Reynolds number varies between 2200 and 6000. According to their numerical results, curved SAH shows better thermal performance measured by the ratio of Nusselt numbers (Nu_{curved}/Nu_{flat}) [3]. Thakur et al. [4] in a numerical effort for the thermo-hydraulic performance of SAH proposed hyperbolic ribs for convection enhancement. They used ANSYS FLUENT 15.0 for CFD analysis of 2D fully-developed steady-state turbulent flow up to Re=10000. They showed that rib geometry results in better performance than rectangular, semicircular, and triangular geometries. Singh [5] proposed a new geometry of arched absorber in plane solar air heaters. He used the ANSYS FLUENT platform with RNG k-ε turbulence model in simulation of the turbulent convection airflow and reported a considerable improvement in Nusselt number for high Reynolds number flows,

The vortex generation technique is one of the efficient methods for heat transfer augmentation, and investigators have examined different types of vortex generators (VGs). Two main categories are stationary and flapping vortex generators. Also, two ways exist to fulfill the vibration of vortex generators; the active method with external power and the passive method with fluid-solid interaction.

As a recent work about the convection enhancement by the passive method, Bayareh et al. [6] simulated the heat transfer over a flat plate with a triangular vortex generator. In that work, the set of governing equations was solved by the CFD technique to determine the velocity and temperature fields inside the laminar convection airflow under a vortex generator. An attempt was made to investigate the effect of the angle of triangular vortex generator on convection enhancement. Numerical results revealed that the longitudinal vortices that have an important impact on the heat transfer become stronger at larger angles of the vortex generator.

The present work focuses on the passive VGs that have been employed for convection enhancement. In the passive vortex generation technique, elastic winglets are located between the airside heat exchanger fins for more heat transfer rate.

Recently, Fluid-Solid-Interaction (FSI) has been a topic of many research works [7]. The oscillating VG and the generated flow vortices cause flow mixing by breaking the thermal boundary layer in convective flows. The oscillation of a micro fin array located on the fin has been examined by Go [8] for heat transfer enhancement in laminar air convection flow, and a 10% increase in the rate of heat transfer was reported due to VG at the same velocity. The installation of multiple elastic structures on the heated surfaces of heat sinks has been discussed by Ali et al. [9, 10], and more rate of convection heat transfer than the single VG was reported. The improvement of heat transfer and its dependency on the material properties of oscillating winglets has been studied by Li et al. [7]. Three VGs with different stiffness were examined and compared for airside heat transfer augmentation. In that study, the flow equations and the equation that governs the VG vibration were solved by the finite volume method using the COMSOL-software for Multi-physics simulation. Numerical results demonstrated that the vortex generator with E=1 MPa causes the maximum rate of heat transfer.

The mixing effect and heat transfer enhancement by multiple flags in a laminar convection flow was studied numerically by Ali et al. [10]. The flexible flags were installed on two heated channel walls in different locations. To solve the governing equations, including the FSI, the ANSYS Fluent software was used. Numerical results showed that mixing is enhanced for larger flaps displacement, such that 99% improvement was seen in the rate of the mixing process. The performance of flag vortex generators in increasing heat transfer rate in convection duct flow was studied experimentally by Kristoffer et al. [11]. In that study, the heat transfer characteristics of turbulent convection airflow under the presence of a flapping flag as a VG were investigated. Also, the influences of channel geometry, flag material properties, and flow conditions on the resulting heat transfer behavior of the system were thoroughly explored. An important finding revealed that the oscillation of the flapping flag in the convection flow enhances the flow turbulence levels and the value of the convection coefficient.

However, the blockage effect of flapping winglets and their related pressure drop in convection flow is crucial during the development of the thermal process,

but the improvement of heat transfer and the energy loss and pumping power must be considered simultaneously, in achieving the high performance. In this regard, the present study focuses on a trade-off between the air pressure drop penalty and the heat transfer enhancement by using highly flexible thin winglets with very large deformation and bending due to FSI. Excessive winglet bending causes a considerable decrease in the value of pressure drop due to two different factors. The first is decreasing in flow obstruction (blockage effect) due to the huge bending of the high elastic thin VG that leads to a lower blockage ratio. The second is the aerodynamic shape of the curved winglet when it bends back a lot. It is expected that the vibration of VG under these conditions enhances the convective heat transfer with small mechanical energy loss .

To materialize this aim, the present study introduces a highly elastic thin winglet as a vortex generator inside a 2-D laminar convection airflow in a heat sink with constant fin temperature to have a more cooling rate. A comprehensive transient thermo hydrodynamic analysis is done by numerical solution of the flow equations, while considering the FSI approach in unsteady condition by the FEM. It should be mentioned that several test cases were simulated for reaching this situation, such that the winglet vibrates in its flapping mode while it is under a large bending. Then the values of VG length, thickness, inclined angle, and stiffness were chosen accordingly. Besides, extensive comparisons were made to show the positive effect of high flexible VG and its pros and cons with its original version; the conventional clean duct, and its main competitor; the rigid vortex generator.

THEORY

The geometry problem with details is shown in Figure 1. The length of high flexible thin elastic sheet attached to the lower fin is defined by L_{VG}. The leading edge of VG is clamped at the bottom of fin surface, and the trailing edge is free with the inclination angle $\beta = 40^0$. The axial position of the clamped leading edge, which is shown by x_0, is equal to 30 mm. The channel height and length are H=20 mm and L=250 mm, respectively. The laminar airflow enters with a fully developed velocity profile which has a parabolic distribution with the maximum velocity of 0.5 m/s. The temperature of airflow at the inlet section is T_{in} =293 K, and the hot surfaces of the fins are at T_w = 433 K. The VG information and characteristics are given in Table 1. A schematic of the deformed shape of VG and its domain of vibration is also drawn in Figure 2 for having a clear image of flapping mode of winglet. As noted before, the main aim of present work is to provide the flapping mode of VG, while it gets a large deformation that makes its profile from the bluff shape into an aerodynamic configuration for lowering the blockage effect, while it vibrates with large displacement.
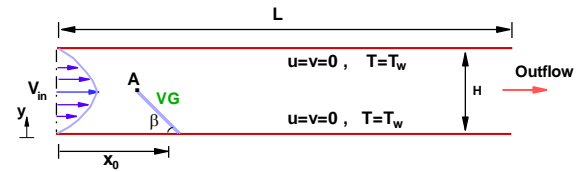

Figure 1. Geometry of heat sink with flapping VG

Table 1. VG information and properties

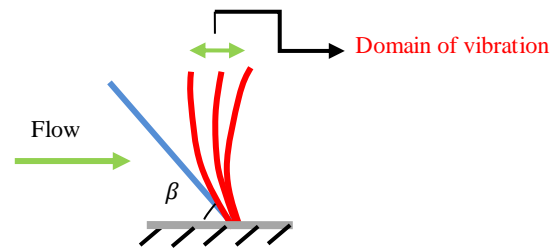| Parameter	Value
Thickness	0.6 mm
Length	13 mm
Attacked angle	40°
Young modulus	0.01 MPa
Poison ratio	0.4
Density	1000 kg/m³

Figure 2. A schematic of VG flapping mode and its deformed shape

Governing equations

The set of governing equations for transient Newtonian incompressible laminar airflow consists of the conservation of mass, momentum and energy, which is coupled with the vibration of VG through Fluid-Solid-Interaction (FSI) is presented as follows:

$$\frac{\partial u}{\partial x} + \frac{\partial v}{\partial y} = 0 \tag{1}$$

$$\rho\left(\frac{\partial u}{\partial t} + u\frac{\partial u}{\partial x} + v\frac{\partial u}{\partial y}\right) = -\frac{\partial P}{\partial x} + \mu\nabla^2 u + F_{ext,x} \tag{2}$$

$$\rho\left(\frac{\partial v}{\partial t} + u\frac{\partial v}{\partial x} + v\frac{\partial v}{\partial y}\right) = -\frac{\partial P}{\partial y} + \mu\nabla^2 v + F_{ext,y} \tag{3}$$

$$\frac{\partial T}{\partial t} + u\frac{\partial T}{\partial x} + v\frac{\partial T}{\partial y} = \alpha.\nabla^2 T \tag{4}$$

In momentum equations, F_{ext} is the external force on fluid due FSI. In addition to the large deformations of VG due to FSI forces from convective air flow, its movement interacts with surrounding, such that this interaction also exerts surface force on the convective air flow. In computational fluid dynamic, this situation is called the two-way modeling [12].

The equation of motion for flapping VG can be written as follows [13]:

$$(\lambda + \mu_s)\frac{\partial}{\partial x_i}\left(\frac{\partial U_{sj}}{\partial x_i}\right) + \mu_s\frac{\partial}{\partial x_j}\left(\frac{\partial U_{si}}{\partial x_j}\right) == \rho_s \ddot{U}_{s\,i} \qquad (5)$$
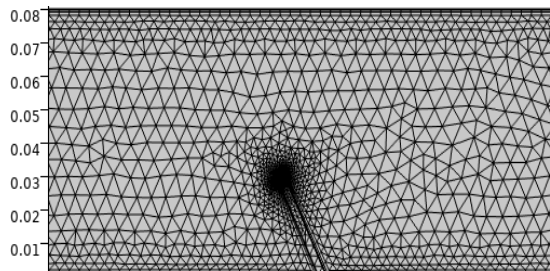
where, U_{si} is the displacement vector. More details about the equation of motion are given by Li et al. [7]. Also, the complete FSI formulation that leads to the computation of external forces in the momentum equation which is provided by the COMSOL software Multiphysics simulation [14].

Grid study
Although the channel has a rectangular shape and the mapped mesh is the best choice for discretization, the unstructured triangular grids were used for the two-dimensional geometry of the channel, because of the VG. The mesh was refined to precisely capture the high gradient of dependent variables near the walls, especially around the vibrating winglet. A schematic of the grid nodes is shown in Figure 3. To find an optimum number of elements for having the grid-independent solution, a grid study was done. The results are tabulated in Table 2, and the average values of the Nusselt number on the lower wall, which are also the time average values during a full period of oscillation at the flapping mode, are reported at different mesh sizes. As seen, the relative error concerning the previous step goes down as the number of elements increases such that at 12440 nodes, the value of relative error becomes about 1%. Hence, this optimum grid size with 12440 elements and average quality of 0.93 is used in all subsequent calculations [14].
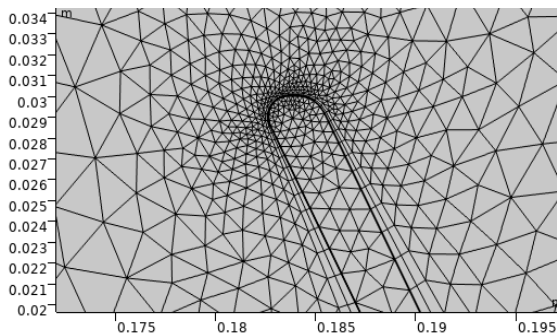
Table 2. Effect of grid size on the converged solution

Mesh	No. of elements	Average Nu	Error
Mesh-1	5340	14.03	-
Mesh-2	8500	14.53	3.5%
Mesh-3	10786	14.93	2.7%
Mesh-4	12440	15.10	1.1%
Mesh-5	14470	15.17	0.5%

Validation
In the present study for validation, as a test case, a laminar convection airflow in a rectangular duct with two heated walls and under the presence of a thin elastic winglet attached to the lower wall was simulated. This problem was also solved by Li et al. [7] with the numerical method. The same number of grid nodes and configuration was used in the present simulation as it was reported in the literature [7]. The role of flapping VG is the vortex generation and mixing process that finally results in convection enhancement. The average value of the Nusselt number along the lower wall at different values of the Reynolds numbers and VG's modulus of elasticities are plotted in Figure 4. An increasing trend for convection coefficient is shown with Re for all values of the module of elasticity. The rigid VG was also included in the simulation. The minimum value of convection coefficient takes place for rigid winglet and the maximum one for elastic agitator with E=1 MPa. A very good agreement was found between our FEM simulation and the findings by Li et al. [7]. Because the flexibility of VG has a considerable influence on its movement and the flow field, the good consistencies between the present findings and numerical results reported by Li et al. [7] showed the reliability of all involved techniques.

In the second test case, the bending angle of a flexible flag in an incoming poiseuille flow was computed and compared with theoretical finding by Wang et al. [15]. In
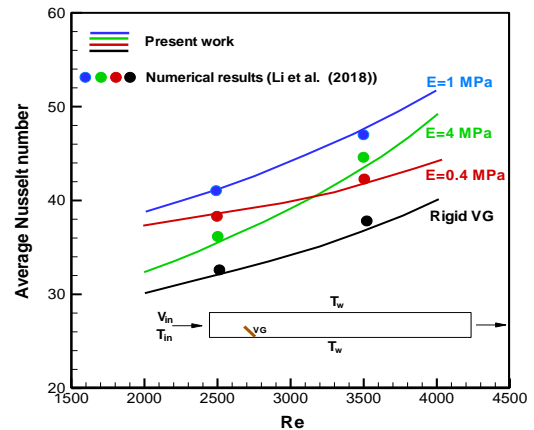

a) High enlarged discretized domain near to VG

b) Grids inside the duct including the vortex generator

Figure 3. The unstructured triangular mesh

Figure 4. Average value of Nu on the lower wall and comparison with the findings reported in literature [7]

that study, the fluid-solid interaction and dynamic of a flexible flag was modeled by the immersed boundary method. The bending angle of deflected flag as a function of bending rigidity at Re=80 is computed and plotted in Figure 5. As shown, the bending angle has a decreasing trend as the flag rigidity gets higher values. The consistency between the results shown in Figure 5 reveals the validity of the present simulation.

Dynamics of flexible vortex generators

The flexible elastic sheet as a VG displays three different motions including the flapping mode, the fully deflected mode and finally the irregular mode depends on the relationship between the hydrodynamic and the restoring forces in the flow field. The VG in the flapping mode displays a regular and continuous movement as it is desired in convection enhancement. In the fully deflected mode, the VG is initially deflected by the hydrodynamic forces, after which it reaches to a stationary position. The VG in irregular mode displays irregular oscillations with small amplitude. As the mixing rate and the convection enhancement takes place by the VG in its flapping mode with high amplitude and frequency, the VG geometrical factors, its inclination angle and the amount of Young modulus were selected to achieve this goal. In Figure 6, the x-displacement of point A on the tip of VG during the time $0 \le t \le 10\ s$ is shown. As seen, the VG reaches to its flapping mode at t=6 s, after which a periodic oscillation with constant amplitude and frequency is seen in the moovement of vortex generator.
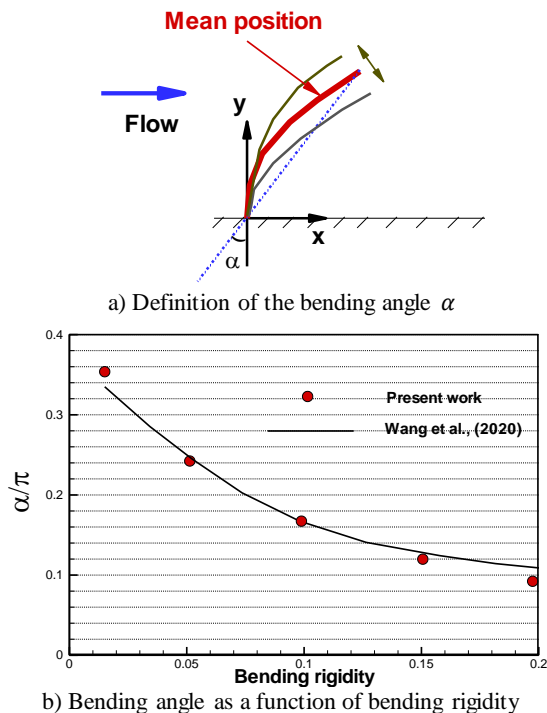

a) Definition of the bending angle α

b) Bending angle as a function of bending rigidity

Figure 5. Variation of the bending angle with the bending rigidity, Comparison with literature [15]
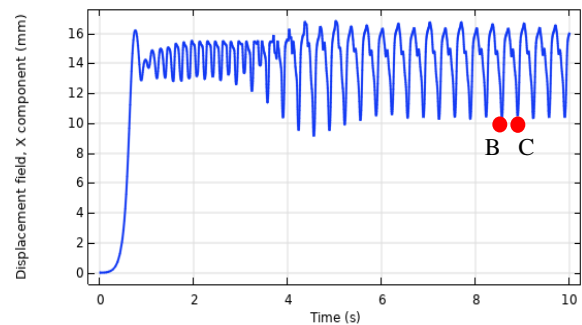

Figure 6. Displacement of point A on the tip of VG with time

RESULTS AND DISCUSSION

The verified numerical technique is employed for solving the FSI coupled with convective heat transfer problem shown in Figure 1 about a heat sink system. In forced convection process, the Reynolds number which is used for determining the regime of fluid flow, is given below:

$$Re = \frac{\rho \bar{V} D_h}{\mu} \qquad (6)$$

In this relation, D_h is the hydraulic diameter is equal to 2H. Here, the value of Reynolds number is kept equal to 900 for all of the test cases. It should be mentioned that the fully turbulence regime begins at Re=10,000 in duct flows [10]. Because the presence of VG in the convective flow, the value of critical Reynolds number becomes lower than this value, although the present Reynolds number is so much smaller. Thereby, all of the simulated test cases are laminar in the heat sink with the elastic agitator.

At first, the contours of velocity magnitude inside the channel at different time steps from t=0 s to t=10 s are drawn in Figure 7. The flow vortices due to the vibration of VG are seen at initial times. These recirculated zones are detached from the VG and move along the channel such that the moving arranged rows of vortices are transported toward the outlet section by progressing in time. In all captured moments, the moving regions with high local values of air velocity can be recognized inside the flow field. This phenomenon is known as the main factor for mixing and heat transfer enhancement. The repeated pattern at t=6 s, after which a periodic behavior takes place, is called the periodic steady state (PSS).

Figure 8 displays the temperature contours along the heat sink fin at different time steps up to the periodic steady state. For all captured moments, high-temperature regions near the heated fin surfaces and also inside the recirculated zones downstream of the flapping VG are shown in Figure 8. The mixing process due to the vortex generator that breaks the temperature boundary layer and increases the heat transfer rate is also depicted in this figure.

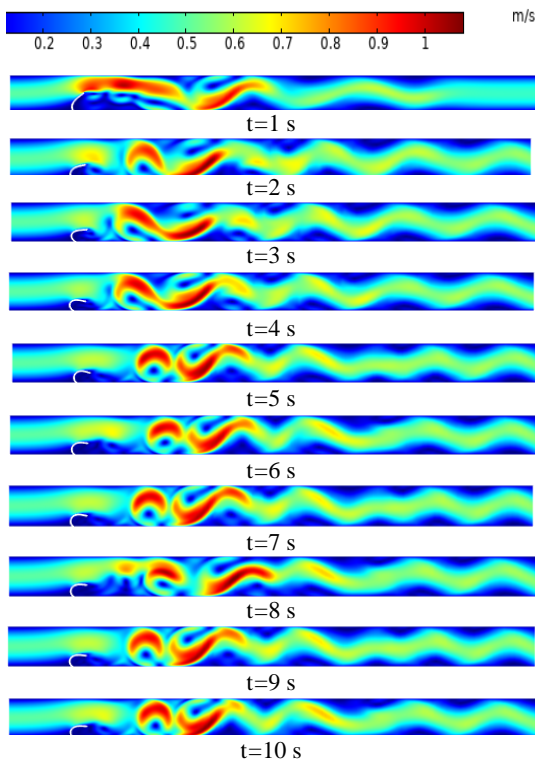As shown before in Figure 6, the vortex generator reaches its flapping mode at t=6 s after which a periodic

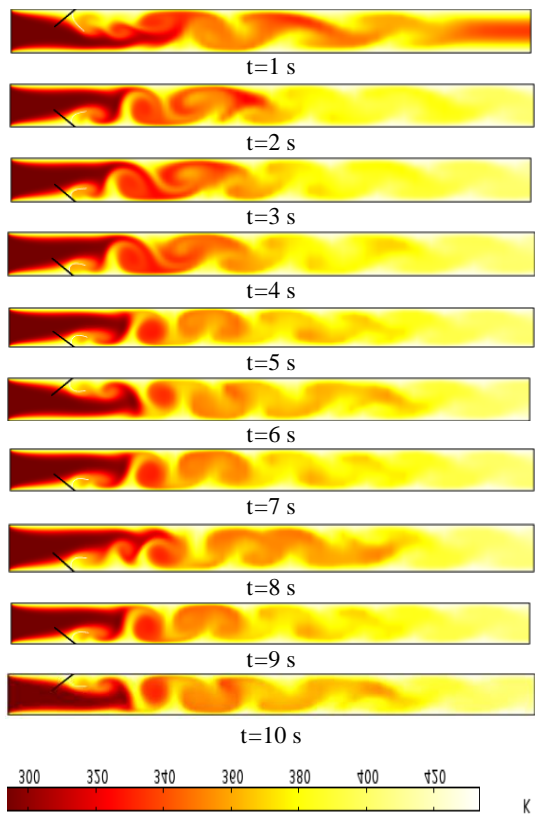**Figure 7.** Velocity contours with flapping VG at different times

Figure 8. Temperature contours with flapping VG at different time

behavior is provided for the VG movement. At the equilibrium state of the flapping mode (zero amplitude), the x-displacement of point A on the tip of VG is equal to 12.8 mm, and the vibration takes place with an amplitude of 2.8 mm. For having a clear image of the flapping mode, the deformed shapes of VG are drawn in Figure 9 during a time period $\tau = 0.33\ s$ from point B to C (Figure 6) at seven different time steps. As seen in all states, the VG has a deformed aerodynamic shape and a convex profile against the airflow.

The pressure field in the airflow is investigated in Figure 10 by plotting the isobars at different times up to t=10 s. The high blockage effect of VG at early timed while the VG has a bluff shape is shown in this figure. But with progressing in time, the large deformation of VG provides an aerodynamic shape for the winglet, resulted in a low blockage effect. The flow vortices due to flapping VG as the regions with a low pressure are shown in Figure 10.
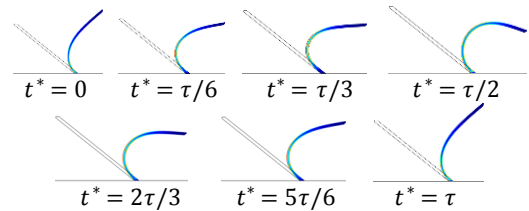

Figure 9. The movement of VG and its deflected shape during a time period of flapping mode ($0 \leq t^* \leq \tau$)
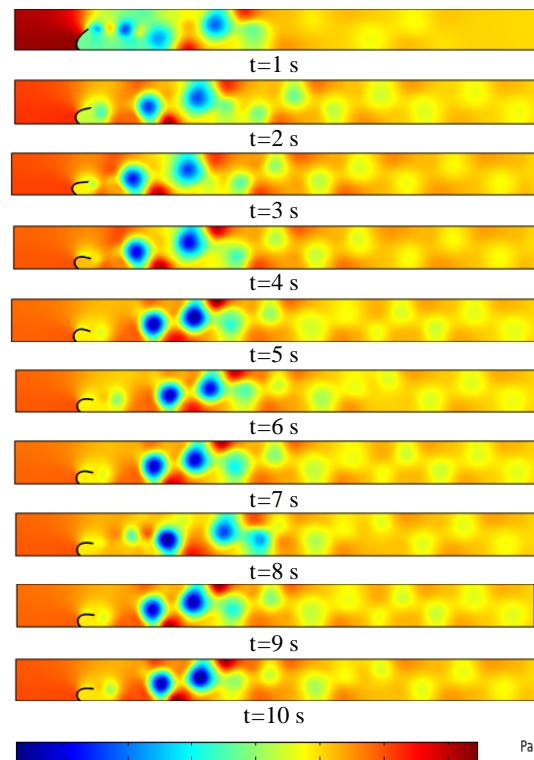

Figure 10. Pressure contours with flapping VG at different time

The variation of air outlet temperature with time is drawn in Figure 11. This figure depicts a rapid air temperature increase at early time after which an oscillation with high frequency is seen for the air outlet temperature that finally converts to a period behavior after t=6 s.

The air bulk temperature distribution at periodic steady conditions along with the axial direction is plotted in Figure 12. It shows how the convection flow is heated along the heat sink by convection heat transfer with the hot fins. The air temperature distribution has several local maximum and minimum points due to the flow vortices. For more study about the effect of VG on heat transfer enhancement, the distributions of Nusselt number on the lower and upper fin surfaces are presented in Figure 13. The mixing effect of VG that breaks the thermal boundary layers and causes several jumps in convection coefficient along the heated surface is seen.
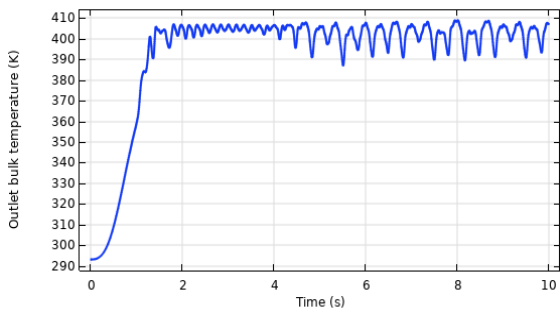
The temperature and pressure fields at steady conditions inside the heat sink with rigid winglet and clean duct are plotted in Figures 14 to 16. It is realized that in the case of rigid winglets and also for clean heat sink, there are not any flow vortices inside the convection flow; such that the existence of a thick thermal boundary layer leads to a low rate of heat transfer from the heated fins towards the core of airflow. The pressure contours plotted in Figure 16 shows high blockage effect of rigid winglet that resulted in more pumping power. One can find that the amount of pressure drop through the heat sink with rigid winglet is four times the clean duct pressure loss. It is due to the bluff shape of the rigid winglet and the high blockage effect of this element.

In order to compare the performances of flapping VG with the rigid winglet and also with clean heat sink, the air bulk temperature distributions along the axial direction and also the variations of Nusselt number along the upper fin surface for three test cases are drawn in Figures 17 and 18. As understood, the elastic VG has a significant positive influence on convection coefficient and the rate of heat transfer between the working gas and heated surface. Besides, it is seen that the test case with

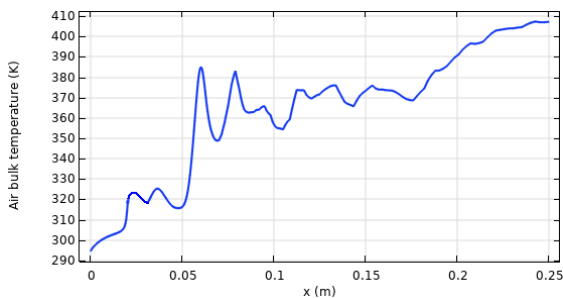**Figure 11.** Variation of air outlet temperature with time

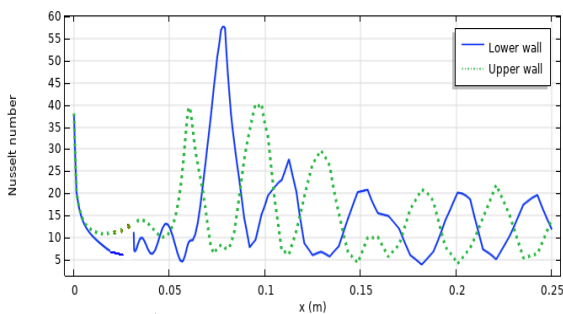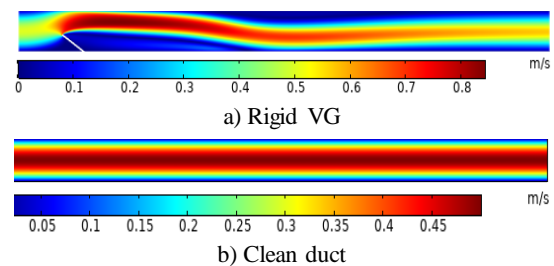**Figure 12.** Air bulk temperature distribution along the axial direction

Figure 13. Variations of Nusselt numbers on the lower and upper fin surfaces

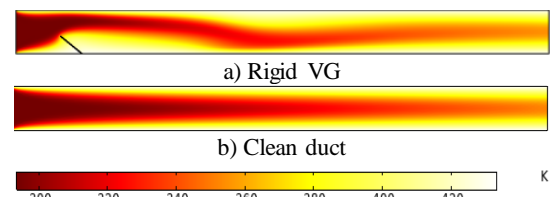**Figure 14.** The contours of velocity magnitude inside the heat sink

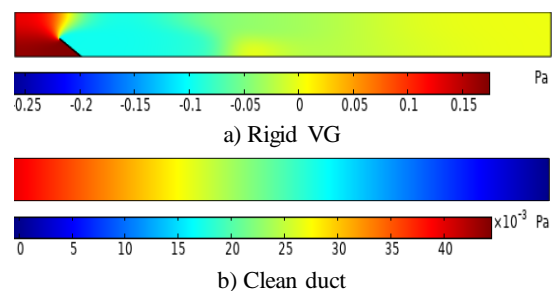**Figure 15.** The contours of temperature inside the heat sink

Figure 16. The contours of pressure inside the heat sink

rigid winglet and the clean heat sink have similar thermal behaviors and cooling effects, as they have the same air outlet temperature.

In Figure 19, the main goal of present study, which is using high elastic VG with a small blockage effect is verified by plotting the air pressure distributions along with the heat sink for the flexible and rigid VGs as well as the clean heat sink. As the system in its semi steady state has a periodic behavior with the time period of $\tau = 0.33\ s$, the value of air pressure in Figure 19 is the time average of this parameter during a full period of oscillation. As expected, the minimum pressure drop belongs to the clean heat sink with, $\Delta p = 0.06\ Pa$, and the heat sink with rigid winglet has the maximum pressure drop with, $\Delta p = 0.15\ Pa$, while this value is reduced for high elastic VG about 33%.
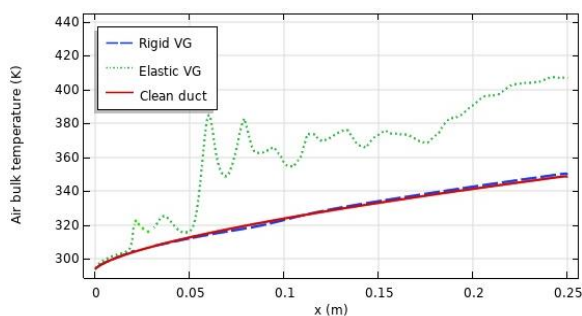

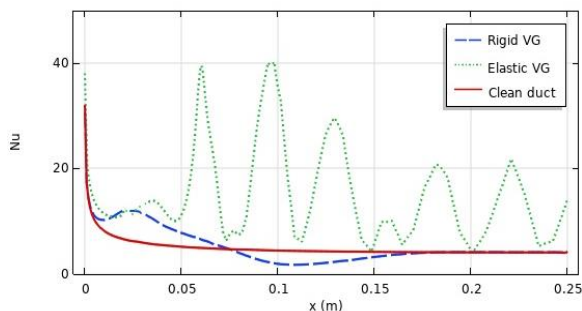**Figure 17.** Distributions of air bulk temperature along the heat sink

Figure 18. Variations of Nusselt number along the upper fin surface
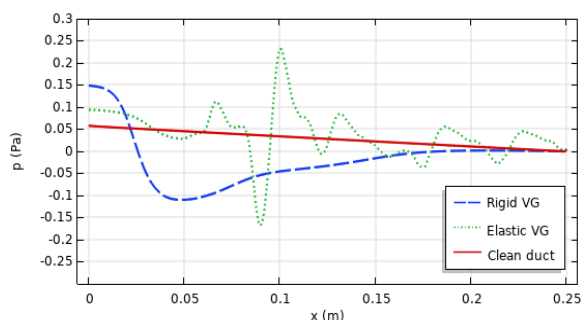

Figure 19. Air pressure distributions along the heat sink

CONCLUDING REMARKS

The main defect of the vortex generation technique in convection enhancement is its pressure drop. In this study, a new idea of employing a very high elastic vortex generator to increase the rate of heat rejection in an airside heat sink with low-pressure loss was examined by a theoretical method. Large deformation of elastic VG due to the FSI force converts its shape from the bluff configuration into an aerodynamic shape with small resistance against the convection flow. The vibration of thin VG with high amplitude leads to flow mixing that finally results in convection augmentation. In the numerical simulation, the set of governing equations for laminar forced convection airflow was solved by the FEM. Numerical results revealed that the vortex generation technique enhances the convection heat transfer by introducing the flow vortices that swept out the temperature boundary layer and cause thermal mixing in the recirculated domain. Also, the large deformation of the VG causes a considerable decrease in its blockage effect and finally in air pressure drop. Numerical findings revealed that the high flexible winglet enhances the rejected heat by 100%, with 33% decrease in pressure drop, when it is compared with the rigid vortex generator at the same air velocity. Besides, the rate of heat rejection in a clean heat sink (without VG) was found equal to that happens in a heat sink with a rigid winglet. This fact demonstrated the positive effect of flapping VGs in heat transfer enhancement.

REFERENCES

1. Njoku, I.H., and Diemuodeke, O.E., 2021. Techno-economic comparison of wet and dry cooling systems for combined cycle power plants in different climatic zones. *Energy Conversion and Management*, 227, pp.113610. Doi: 10.1016/j.enconman.2020.113610

2. Singh, A.P., and Singh, O.P., 2019. Thermo-hydraulic performance enhancement of convex-concave natural convection solar air heaters. *Solar Energy*, 183, pp.146–161. Doi: 10.1016/j.solener.2019.03.006

3. Singh, A.P., and Singh, O.P., 2020. Curved vs. flat solar air heater: Performance evaluation under diverse environmental conditions. *Renewable Energy*, 145, pp.2056–2073. Doi: 10.1016/j.renene.2019.07.090

4. Thakur, D.S., Khan, M.K., and Pathak, M., 2017. Performance evaluation of solar air heater with novel hyperbolic rib geometry. *Renewable Energy*, 105, pp.786–797. Doi: 10.1016/j.renene.2016.12.092

5. Singh, S., 2017. Performance evaluation of a novel solar air heater with arched absorber plate. *Renewable Energy*, 114, pp.879–886. Doi: 10.1016/j.renene.2017.07.109

6. Bayareh, M., Nourbakhsh, A., and Khadivar, M.E., 2018. Numerical simulation of heat transfer over a flat plate with a triangular vortex generator. *International Journal of Heat and Technology*, 36(4), pp.1493–1501. Doi: 10.18280/ijht.360443

7. Li, Z., Xu, X., Li, K., Chen, Y., Huang, G., Chen, C., and Chen, C.-H., 2018. A flapping vortex generator for heat transfer

enhancement in a rectangular airside fin. *International Journal of Heat and Mass Transfer*, 118, pp.1340–1356. Doi: 10.1016/j.ijheatmasstransfer.2017.11.067

8. Go, J.S., 2003. Design of a microfin array heat sink using flow-induced vibration to enhance the heat transfer in the laminar flow regime. *Sensors and Actuators A: Physical*, 105(2), pp.201–210. Doi: 10.1016/S0924-4247(03)00101-8

9. Ali, S., Habchi, C., Menanteau, S., Lemenand, T., and Harion, J.-L., 2017. Three-dimensional numerical study of heat transfer and mixing enhancement in a circular pipe using self-sustained oscillating flexible vorticity generators. *Chemical Engineering Science*, 162, pp.152–174. Doi: 10.1016/j.ces.2016.12.039

10. Ali, S., Menanteau, S., Habchi, C., Lemenand, T., and Harion, J.-L., 2016. Heat transfer and mixing enhancement by using multiple freely oscillating flexible vortex generators. *Applied Thermal Engineering*, 105, pp.276–289. Doi: 10.1016/j.applthermaleng.2016.04.130

11. Gallegos, R.K.B., and Sharma, R.N., 2019. Heat transfer performance of flag vortex generators in rectangular channels.

International Journal of Thermal Sciences, 137, pp.26–44. Doi: 10.1016/j.ijthermalsci.2018.11.001

12. Lee, J.B., Park, S.G., Kim, B., Ryu, J., and Sung, H.J., 2017. Heat transfer enhancement by flexible flags clamped vertically in a Poiseuille channel flow. *International Journal of Heat and Mass Transfer*, 107, pp.391–402. Doi: 10.1016/j.ijheatmasstransfer.2016.11.057

13. Le Tallec, P., and Mouro, J., 2001. Fluid structure interaction with large structural displacements. *Computer Methods in Applied Mechanics and Engineering*, 190(24–25), pp.3039–3067. Doi: 10.1016/S0045-7825(00)00381-9

14. Dickinson, E.J.F., Ekström, H., and Fontes, E., 2014. COMSOL Multiphysics®: Finite element software for electrochemical analysis. A mini-review. *Electrochemistry Communications*, 40, pp.71–74. Doi: 10.1016/j.elecom.2013.12.020

15. Wang, S., Ryu, J., Yang, J., Chen, Y., He, G.Q., and Sung, H.J., 2020. Vertically clamped flexible flags in a Poiseuille flow. *Physics of Fluids*, 32(3), pp.031902. Doi: 10.1063/1.5142567

Persian Abstract

چکیده

در این پژوهش، استفاده از یک بالک نازک بسیار منعطف به عنوان مولد گردابه به منظور افزایش نرخ انتقال حرارت جابجایی در داخل یک چشمه حرارتی مورد تجزیه و تحلیل قرار گرفته است. وجود گردابه در جریان واختلاط ناشی از آن، شکست لایه مرزی حرارتی را باعث شده و نهایتاً افزایش شدت انتقال حرارت جابجایی را به دنبال دارد. خمش زیاد بالک منعطف در حین نوسان، میزان انسداد جریان و در پی آن افت فشار ایجاد شده را کاهش داده و این رفتار مورد توجه خاص بوده است. در شبیه‌سازی مسئله باروش المان محدود، معادلات حاکم در شرایط گذرا شامل پیوستگی، ممنتم و انرژی با در نظر داشتن نیروهای بین سازه و سیال به صورت دو طرفه، توسط نرم‌افزار کامسول حل عددی شده است. نتایج بدست آمده گواه بر خمش زیاد مولد گردابه در حال نوسان بوده و در حین این که ضریب انتقال حرارت جابجایی و نرخ انتقال حرارت را به مقدار قابل ملاحظه‌ای زیاد می‌کند به واسطه داشتن شکل ایرودینامیکی، در کاهش افت فشار جریان نیز موثر عمل می‌نماید، به طوری که مقایسه عملکرد این بالک منعطف با نوع صلب آن، ۱۰۰٪ افزایش نرخ انتقال حرارت و ۳۳٪ کاهش افت فشار را نشان می دهد.